

44. K. W. Street, Jr., W. E. Acree, Jr., J. C. Fetzer, P. H. Shet, and C. F. Poole, *Appl. Spectrosc.* **43**, 1149 (1989).
45. S. A. Tucker, L. E. Cretella, R. Waris, K. W. Street, Jr., W. E. Acree, Jr., and J. C. Fetzer, *Appl. Spectrosc.* **44**, 269 (1990).
46. U. Breymann, H. Dreeskamp, E. Koch, and M. Zander, *Chem. Phys. Lett.* **59**, 68 (1978).
47. S. A. Tucker, J. M. Griffin, W. E. Acree, Jr., P. P. Mulder, J. Lugtenburg, and J. Cornelisse, *Analyst (Cambridge, U.K.)* **119**, 2129 (1994).
48. L. C. Sander and S. A. Wise, *Polycyclic Aromatic Hydrocarbon* (NIST Special Publication 922, Washington, 1997).
49. S. L. Murov, I. Carmichael, and G. L. Hug, *Handbook of Photochemistry* (Marcel Dekker, New York, 1993), 2nd ed.

Forensic Analysis of Single Fibers by Raman Spectroscopy*

JASON V. MILLER[†] and
EDWARD G. BARTICK[‡]

Department of Forensic Sciences, The George Washington University, Washington, District of Columbia 20052 (J.V.M.); and Forensic Science Research Unit, FBI Academy, § Quantico, Virginia, 22135 (E.G.B.)

Index Headings: **Forensic analysis; Fibers; Raman spectroscopy; Raman microscopical analysis; Raman microprobe; Raman microspectroscopy.**

INTRODUCTION

Polymeric identification is an important step in the forensic analysis of transferred fibers collected as evidence. In addition to physical and optical comparison of known and questioned fibers, polymeric identification of the fiber provides the forensic scientist with information on which to base conclusions, such as transfer behavior and prevalence in the community.¹ After collecting potentially significant fibers and screening them with a stereo microscope, they are mounted on glass slides for further examination by comparison, polarized light (PLM), and fluorescence microscopes. Optical properties such as index of refraction, birefringence, and optical sign of elongation are used to determine the generic class of the fiber. As fiber technology has progressed, new generic and subgeneric classes of fibers have been developed. PLM cannot be used to differentiate between subgeneric classes; therefore, a method with additional discrimination is nec-

essary to more fully characterize the chemical composition of fibers.

Microscopical analysis by FT-IR spectroscopy has been the preferred method for obtaining additional information on the polymeric composition of a fiber.²⁻⁴ It allows unequivocal determination of the generic class and frequently permits subclassification.^{5,6} FT-IR analysis cannot be conducted while the fiber is mounted due to the strong absorption of infrared (IR) radiation by glass. The fiber must be removed from the slide and rinsed to clean off the mounting medium before preparing the fiber. This increases sample preparation time and the chance for sample loss.

Glass produces little response to Raman spectroscopy. Therefore, Raman analysis of fibers can be conducted while the fiber remains mounted on a glass slide under coverslips. The theoretical beam width of the laser is 0.8 μm ; thus, Raman will potentially permit measurement of microfibers used in some fabrics in the current market. The samples do not need to be thinned or flattened, as with IR, because the photons are scattered from the surface and not transmitted through the sample.

The current literature contains limited reports and citations on the use of Raman microprobe spectroscopy for forensic analysis of fibers. Research by Lang et al.⁷ has shown that it is possible to scan fibers while they are taped onto a glass slide. By the same sample preparation method, Keen et al.⁸ have shown that it is possible to differentiate between several generic and subgeneric classes of fibers. This report will demonstrate that it is possible to scan through a glass coverslip and mounting medium to obtain polymeric identification of nondyed fibers.

EXPERIMENTAL

Undyed fiber samples were obtained from the Collaborative Testing Services (CTS) (Herndon, VA) 1987 Collection and from an FBI collection acquired from manufacturers. Three sample preparation methods were used: (1) fibers were taped directly to glass microscope slides for analysis, (2) samples were taped to the shiny side of aluminum foil covering microscope slides, and (3) samples were mounted in Permount, produced by Fisher Scientific (Pittsburgh, PA), under glass coverslips on microscope slides. Including the subclasses, a total of 70 fiber types were analyzed by these methods.

Raman spectra were collected using a Renishaw (Gloucestershire, United Kingdom) Model 2000 spectrograph attached to an Olympus (Melville, NY) BHSM metallurgical microscope. A 785 nm, 300 mw, continuous wave, wavelength-stabilized laser diode (SDL, San Jose, CA) was used as the excitation source. For all scans, a 50 \times microscope objective was used that produced a theoretical 0.8 μm spot size on the sample. Using 180 $^\circ$ back-scattering geometry, the scattered light was collected by the objective and passed through a holographic notch filter to remove the Rayleigh line. The detector was a thermoelectrically cooled charge-coupled device (CCD) detector of 576 \times 384 pixels. Spectra were collected in the range of 200 to 2000 cm^{-1} except for acrylic and modacrylic fibers, which were collected from 200 to 2400 cm^{-1} . Spectral acquisition, presentation, and analysis were performed with the Renishaw WIRE and

* The bases of this note was presented at the 26th Annual Conference of the Federation of Analytical Chemistry and Spectroscopy Societies (FACSS), Vancouver, British Columbia, Canada, Oct. 24-29, 1999.

[†] Current Address: Explosives Unit, Laboratory Division, Federal Bureau of Investigation, 935 Pennsylvania Avenue, N.W., Washington, DC 20535.

[‡] Author to whom correspondence should be sent.

[§] This is publication number 01-21 of the Laboratory Division of the Federal Bureau of Investigation. Names of commercial manufacturers are provided for identification only and inclusion does not imply endorsement by the Federal Bureau of Investigation.

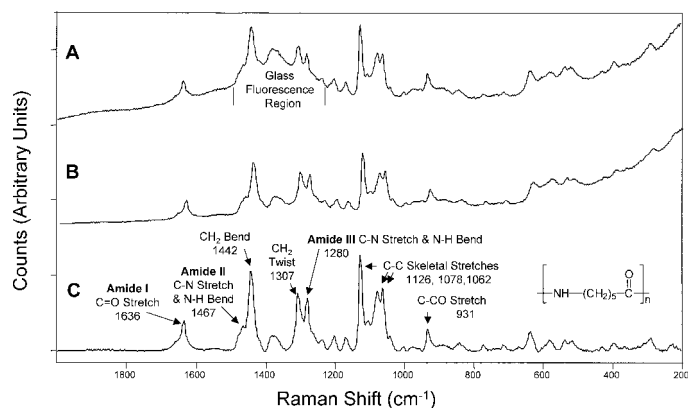


FIG. 1. Raman spectra of a nylon 6 fiber on different mounts. (A) nylon 6 taped on a glass slide; (B) nylon 6 taped on an aluminum foil slide; (C) nylon 6 on an aluminum foil slide after baseline flattening.

GRAMS[™]/32C (Galactic Industries, Salem, NH) software. The spectra were acquired using scan time settings of 120 s for the aluminum foil slides and four coadded scans of 30 s for the Permout-mounted slides. Total analysis time in both cases was approximately eight minutes, because the software time settings are for the portion of the spectrum for each grating position. The gratings are moved incrementally to cover the spectral range specified. The portions of the spectrum are digitally stitched together to complete the total spectral range covered. The instrument was calibrated for frequency daily to within one wavenumber of naphthalene. Spectra of a blank glass slide and Permout between a coverslip and a glass slide were collected daily for subtraction from the Permout-mounted fiber spectra. No instrument response corrections were made.

RESULTS AND DISCUSSION

Fibers were initially taped on top of glass slides and analyzed directly where there was no tape; therefore, no interference from the tape occurred. Figure 1A shows a spectrum of a nylon 6 fiber that is typical of fibers taped directly on a glass slide. Fluorescence from the glass slide produces a large broad underlying peak near 1400 cm^{-1} . To remove the interference contributed by the peak, a background spectrum of the glass slide alone must be subtracted from the fiber spectrum acquired on the glass. The use of aluminum foil to back the fiber eliminated the fluorescence of glass and the subtraction step. Figure 1B shows a spectrum of a nylon 6 fiber taped on an aluminum foil-covered slide. Note that the underlying broad peak around 1400 cm^{-1} is now absent. After baseline flattening, the high-quality spectrum in Figure 1C results. The spectrum is shown with major peak assignments as described by Hendra et al.⁹ who analyzed nylon pellets using an FT-Raman system. The peak frequencies, obtained by the Grams[™] peak-picking routine, are within one wavenumber of Hendra's results, with the exception of the 1078 cm^{-1} peak, which is two wavenumbers different.

Next, studies were conducted on fibers mounted under glass coverslips. Figure 2A shows a spectrum of a nylon 6 fiber typical of fibers mounted in Permout. Along with the large broad peak near 1400 cm^{-1} due to the fluores-

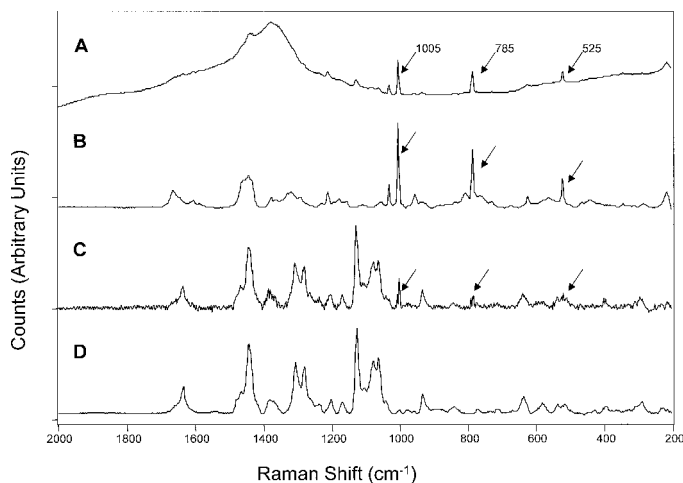


FIG. 2. Raman spectra of a nylon 6 fiber mounted on a glass slide in Permout with a coverslip. (A) nylon 6 mounted in Permout (arrows show major Permout peaks); (B) Permout on aluminum foil; (C) nylon 6 mounted in Permout after subtraction of Permout and glass slide and baseline flattening plotted full scale (arrows show subtraction artifacts); (D) nylon 6 spectrum obtained on aluminum foil-covered slide.

cence of glass, several additional peaks from the Permout are evident. A spectrum of neat Permout is shown in Fig. 2B with the major peaks near 1005 , 785 , and 525 cm^{-1} . Permout is a formulation of pinene, toluene, and 2,6-di-tert-butyl-P-cresol. A background spectrum taken adjacent to the fiber was subtracted to eliminate the Permout peaks. Often, the broad peak from the glass fluorescence was still present, and a second subtraction of the glass slide was necessary to remove the contribution from the glass. The final spectrum after baseline flattening is shown in Fig. 2C.

Perturbation from intermolecular interaction due to apparent hydrogen bonding between the Permout and the fiber¹⁰ was observed on the final subtraction spectrum shown in Fig. 2C. Artifacts are indicated by arrows where the major Permout bands were subtracted. Hydrogen bonding with the fiber appears to have broadened the Permout bands, thus producing second derivative-shaped curves after subtracting the spectrum of Permout. Attempts to reduce the intensity of these residual bands by changing the thickness compensation factor resulted in negative nylon 6 bands. The bands do not interfere with the interpretation of the spectra and are minimal compared to perturbation effects that are often observed in spectral subtraction calculations.

For comparison, Fig. 2D shows the nylon 6 spectrum obtained on aluminum foil. Raman spectra of fibers mounted in Permout generally have a lower signal-to-noise ratio than those measured on an aluminum foil slide. Nevertheless, characteristic bands are still observable, and the peak frequencies are within one wavenumber when comparing the subtracted Permout slide with the aluminum slide and the spectra obtained by Hendra et al. This is also true after a 13-point Savitsky-Golay smooth is performed on the final spectrum from the glass mount.

Nylon 6,6 is also frequently seen as evidence in forensic laboratories. The ability to distinguish nylon 6 from nylon 6,6 provides an additional subgeneric discriminat-

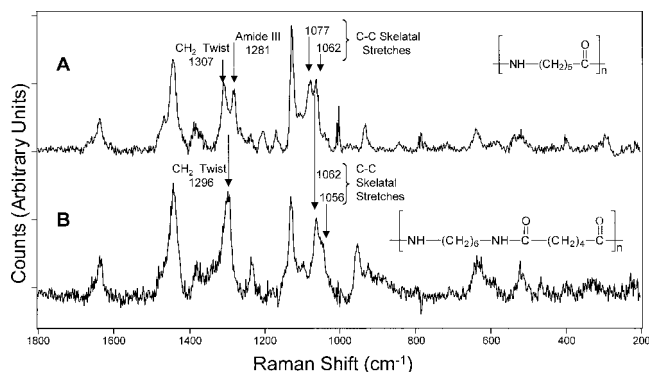


FIG. 3. Comparison of Raman spectra of two nylon fibers mounted in Permount with the distinguishing peaks labeled. (A) nylon 6; (B) nylon 6,6.

ing factor that could prove useful in a forensic investigation. Spectra of nylon 6 and nylon 6,6, acquired in the slide mount, are shown in Figs. 3A and 3B, respectively, with their polymeric structures. The peak assignments used to differentiate between the nylons are listed on the spectra.^{9,11} The nylon 6,6 spectrum does not have an amide III band (C–N stretch and N–H bend) at 1281 cm^{-1} , and the C–C skeletal stretches are shifted from the peak locations in the nylon 6 spectrum.

Since Raman spectroscopy provides information that is complimentary to IR, it is useful to compare the information gained from Raman spectroscopy to that from the IR. Generally, C–C bonds found in the skeletal backbone structure of many polymeric fibers readily polarize and will be good Raman scatterers, producing many characteristic peaks. Likewise, strong dipole moments from functional group vibrations will absorb strongly in the IR. Figure 4 shows IR spectra of nylon 6 and nylon 6,6 in Figs. 4A and 4B, respectively. The two nylon spectra are very similar. The major bands are characteristic for polyamides and make the identification of the generic class a simple task. However, the features distinguishing the sub-generic classes are more subtle. The most convenient way by IR to differentiate between nylon 6,6 and nylon 6 is by the presence of the weak crystalline band near 935 cm^{-1} in the nylon 6,6 spectrum. To determine the differences between the different numbered series of nylons, it is necessary to carefully compare the small skeletal-region bands between 1150–1000 cm^{-1} . When conducting IR spectral searches of nylons, it is necessary to limit the computer search to 1150–900 cm^{-1} to obtain the correct results for the nylon subclasses. Differences are more apparent in the Raman spectra, and they are easier to distinguish.

Acrylic fibers are another important generic class in forensic analysis because these fibers, frequently used in sweaters, can readily transfer during contact.¹² Acrylics are composed of at least 85 percent by weight of polyacrylonitrile along with other comonomers and ionic end groups.¹³ As a result of variations in composition, IR analysis is useful for discriminating over 20 known subclasses. Figure 5 contains four IR spectra of major sub-generic classes of acrylic fibers. The major characteristic spectral feature for acrylics is the nitrile band near 2240 cm^{-1} shown in Fig. 5A of polyacrylonitrile homopolymer. The comonomers shown in Figs. 5B, 5C, and 5D

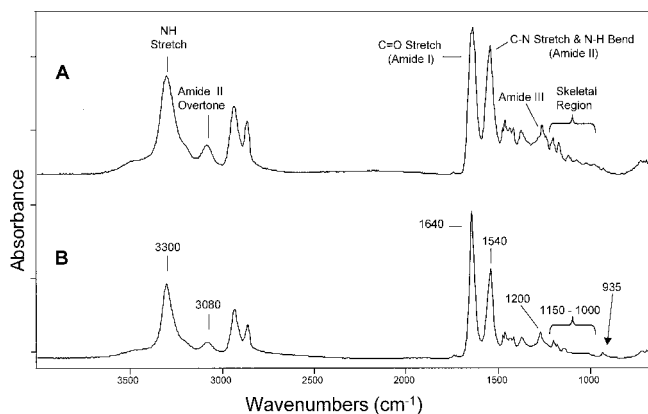


FIG. 4. Infrared spectra of two nylon fibers with the distinguishing peaks labeled. (A) nylon 6; (B) nylon 6,6.

contain carbonyls that absorb near 1730 cm^{-1} . The differentiating features in these spectra lie in the C–O stretching region between 1300–1100 cm^{-1} . Additional comonomers and additives show characteristic features in the IR that permit further discrimination between the subclasses of acrylic fibers.

In comparison to the IR spectra, Raman acrylic fiber spectra, shown in Fig. 6, have only minor notable differences. The nitrile stretch is observable near 2240 cm^{-1} , but the carbonyl and the C–O stretches do not appear in these spectra. Minor variations in band shapes are the only differences. Application of multivariate analysis to Raman spectra may lead to improved discrimination of such spectra, but with the addition of dye features, acrylic fibers are not likely to be subclassified using Raman analysis.

Most other fiber types studied were found identifiable by Raman analysis. An exception is glass fibers on microscope mounts. Glass fibers produce the same fluorescence response in their spectra as the glass coverslips. No other features are observable to identify them as glass fibers. Therefore, Raman analysis is not useful for identifying glass fibers while mounted on microscope slides. In addition to acrylics, saran fibers are the only class that cannot be subclassified by Raman spectroscopy. Sarans differ only in the amount of plasticizer used in the pro-

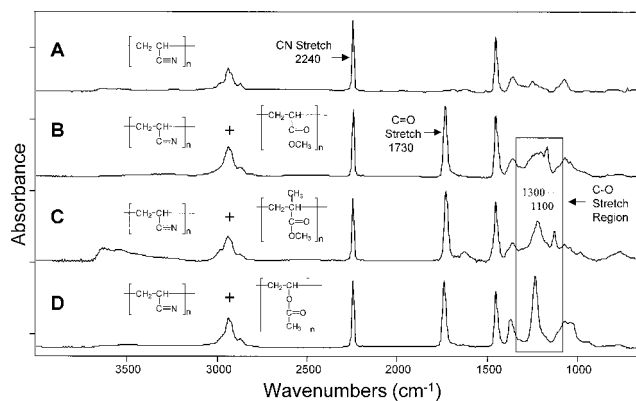


FIG. 5. Comparison of infrared spectra of four major acrylic sub-generic classes. (A) polyacrylonitrile homopolymer; (B) poly(acrylonitrile:methyl acrylate); (C) poly(acrylonitrile:methyl methacrylate); (D) poly(acrylonitrile:vinyl acetate).

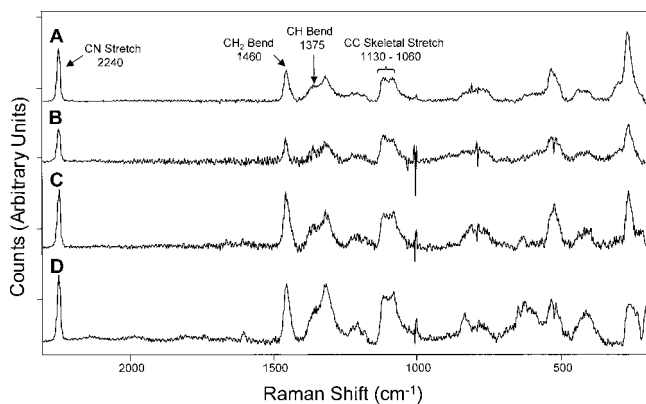


Fig. 6. Comparison of Raman spectra of four major acrylic subgeneric classes. (A) polyacrylonitrile homopolymer; (B) poly(acrylonitrile:methyl acrylate); (C) poly(acrylonitrile:methyl methacrylate); (D) poly(acrylonitrile:vinyl acetate).

duction of the fibers. The ester bands of the plasticizer are not observable in the Raman spectra. Table I shows the generic classes of fibers with the ability to identify generic classes and subclasses of nondyed fibers based

TABLE I. Ability to use IR vs. Raman analysis in fiber class and subclass identification of nondyed fibers.

Fiber class	IR		Raman	
	Class	Subclass	Class	Subclass
Acetate	good	poor/difficult	good	good
Acrylic	good	good	good	poor
Aramid	good	good	good	good
Azlon	good	good	good	good
Fluorocarbon	good	good	good	good
Glass	good	NA ^a	poor	NA ^a
Modacrylic	good	good	good	good
Natural	good	good	good	good
Novaloid	good	NA	good	NA
Nylon	good	good	good	good
Polycarbonate	good	NA	good	NA
Polyester	good	good	good	good
Olefin	good	good	good	good
Rayon	good	NA	good	NA
Saran	good	good	good	poor
Spandex	good	good	good	good
Sulfar	good	NA	good	NA
Vinyl	good	NA	good	NA
Vinyon	good	NA	good	NA

^a NA indicates that there are no subclasses in this generic class.

on IR vs. Raman spectra. The IR and Raman spectra were compared by Miller¹⁴ for the entire 70 fibers analyzed.

CONCLUSION

Raman spectra of single fibers were obtained directly from glass slide mounts; therefore, no additional sample preparation was required after visual light microscopy. Glass fibers are an exception because they cannot be analyzed by this method. Subgeneric identification by Raman analysis was successful for nondyed fibers with the exception of acrylics and sarans. With these fiber classes, spectral differences are too subtle for clear distinction between subclasses, and therefore, IR analysis is recommended for subclassification of acrylics and sarans. A study dealing with Raman analysis of dyed fibers will be addressed in a forthcoming publication.

1. J. Robertson and C. Roux, "From the Crime Scene to the Laboratory", in *Forensic Examination of Fibers*, J. Robertson and M. Grieve, Eds. (Taylor and Francis Inc., Philadelphia, 1999), 2nd ed., Chap. 5, p. 89.
2. M. C. Grieve, "Fibres and Their Examination in Forensic Science", in *Forensic Science Progress*, A. Maehly and R. L. Williams, Eds., (Springer-Verlag, New York, 1990), p. 41.
3. M. W. Tungol, E. G. Bartick, and A. Montaser, "Forensic Examination of Synthetic Textile Fibers by Microscopic Infrared Spectrometry", in *Practical Guide to Infrared Microspectroscopy*, H. J. Humecki, Ed., (Marcel Dekker, Inc., New York, 1995), Chap. 7, p. 245.
4. K. P. Kirkbride and M. W. Tungol, "Infrared Microspectroscopy of Fibres", in *Forensic Examination of Fibers*, J. Robertson and M. Grieve, Eds. (Taylor and Francis Inc., Philadelphia, 1999), 2nd ed., Chap. 8, p. 179.
5. M. W. Tungol, E. G. Bartick, and A. Montaser, *Appl. Spectrosc.* **44**, 543 (1990).
6. M. W. Tungol, E. G. Bartick, and A. Montaser, *Spectrochim. Acta, Part B* **46**, 1535E (1991).
7. P. L. Lang, J. E. Katon, J. F. O'Keefe, and D. W. Schiering, *Microchem. J.* **34**, 319 (1986).
8. I. P. Keen, G. W. White, and P. M. Fredericks, *J. Forensic Sci.* **43**, 82 (1998).
9. P. J. Hendra, W. F. Maddams, I. A. M. Royaud, H. A. Willis, and V. Zichy, *Spectrochim. Acta, Part A* **46**, 747 (1990).
10. T. Hirschfeld and K. Kizer, *Appl. Spectrosc.* **29**, 345 (1975).
11. W. F. Maddams and I. A. M. Royaud, *Spectrochim. Acta, Part A* **47**, 1327 (1991).
12. C. A. Pounds and K. W. Smalldon, *J. Forens. Sci. Soc.* **15**, 17 (1975).
13. M. C. Grieve, *Science & Justice* **35**, 179 (1995).
14. J. V. Miller, Masters Thesis, The George Washington University, Washington, DC (1999).